Reports

Bacterial Motility: Membrane Topology of the *Escherichia coli* MotB Protein

SANG YEARN CHUN AND JOHN S. PARKINSON

The MotB protein of *Escherichia coli* is an essential component of the force generators that couple proton movement across the cytoplasmic membrane to rotation of the flagellar motors. The membrane topology of MotB was examined to explore the possibility that it might form a proton channel. MotB–alkaline phosphatase fusion proteins were constructed to identify likely periplasmic domains of the MotB molecule. Fusions distal to a putative membrane-spanning segment near the amino terminus of MotB exhibited alkaline phosphatase activity, indicating that an extensive carboxyl-terminal portion of MotB may be located on the periplasmic side of the membrane. Protease treatment of MotB in spheroplasts confirmed this view. The simple transmembrane organization of MotB is difficult to reconcile with a role as a proton conductor.

MOTILE CELLS OF *Escherichia coli* and many other bacteria swim by rotating flagellar filaments (*1*). The rotational motion is generated by a motor composed of several dozen different proteins embedded in the cytoplasmic membrane, cell wall, and outer membrane (*2, 3*). Output from the motor is transmitted through a flexible hook to the flagellar filaments, which serve as semirigid propellers. Flagellar motors are powered by proton motive force (*4*) and can rotate in either direction (*5*). Two cytoplasmic membrane proteins, MotA and MotB, play key roles in this process. Mutants defective in either function possess morphologically normal basal bodies but cannot rotate their flagella (*3, 6, 7*). The Mot proteins are generally considered to be the primary energy-coupling devices responsible for converting proton potential into mechanical work. They might, for example, form proton channels in the cytoplasmic membrane that interact with components of the flagellar basal structure and switching apparatus to power the rotational machinery. Determination of the transmembrane organization of MotA and MotB molecules may provide useful clues to understanding their functions. Here, we report genetic and biochemical studies that show that MotB has a simple topology; it crosses the cytoplasmic membrane only once, with the bulk of the molecule located in the periplasmic space. This finding raises the possibility that, rather than acting as a proton conductor, MotB might serve as a structural support that anchors the rotational machinery to the cell wall.

To investigate the membrane topology of MotB, we used the Tn*phoA* transposon (*8*) to construct *motB-phoA* gene fusions in which the catalytic domain of alkaline phosphatase (PhoA) was joined to various lengths of the NH_2-terminus of MotB. Since alkaline phosphatase must be exported to the periplasm to acquire enzymatic activity, fusion of PhoA to domains of MotB that are normally located on the periplasmic side of the membrane should result in a Pho^+ phenotype, whereas fusion to cytoplasmic regions of MotB should produce a Pho^- phenotype (*9*). We examined 22 independent, Pho^+ *motB*::Tn*phoA* insertions and found 14 different fusion sites in the MotB molecule (Fig. 1). As was expected, these Pho^+ fusions joined the *motB* and *phoA* coding sequences in the proper reading frame. In contrast, several Pho^- isolates chosen as controls either had the *phoA* coding sequence joined out of frame or in inverted orientation. The Pho^+ isolates exhibited 20 to 50 times more alkaline phosphatase activity than these controls.

Plasmid-encoded proteins from each of the Pho^+ isolates were labeled with [^{35}S]-methionine and analyzed by electrophoresis in denaturing polyacrylamide gels. In every case the size of the hybrid protein corresponded closely to that predicted from the location of the fusion point in the *motB* and *phoA* coding sequences (*10*), suggesting that MotB-PhoA hybrids are not readily degraded, even though other PhoA fusion proteins undergo proteolytic processing (*8, 9, 11*). Since native PhoA functions as a dimer (*12*), these findings imply that MotB-PhoA molecules are capable of forming dimeric or higher order complexes.

The MotB protein is 308 amino acids in length and contains four moderately hydrophobic segments, which might conceivably influence MotB topology by interacting with the membrane (*13*) (Fig. 1). None of these segments resembles a cleavable signal sequence, and comparison of in vivo and in vitro translation products has indicated that MotB molecules do not undergo extensive proteolytic processing (*14*). The first hydrophobic region (segment A, residues 28 to 49) resembles typical membrane-spanning sequences in overall hydrophobicity, length, and possible α-helical structure. It is flanked on the COOH-terminal side by segment B (residues 55 to 72), a less hydrophobic region. Stader *et al.* (*13*) have suggested that hydrophobic segments A and B both traverse the membrane, leading to the topology shown in Fig. 2 (I), in which most of the MotB polypeptide is located in the cytoplasmic compartment. The distribution of Pho^+ *motB*::Tn*phoA* insertion points argues against this model (see Fig. 1). Rather, it appears that much of MotB may reside on the periplasmic side of the membrane, since fusion of PhoA to many different points in the molecule yielded enzymatically active hybrids. These findings suggested an alternative model of MotB topology, depicted in Fig. 2 (II), in which only hydrophobic segment A spans the membrane, leaving the COOH-terminus of the molecule in the periplasm.

To distinguish the two topology models

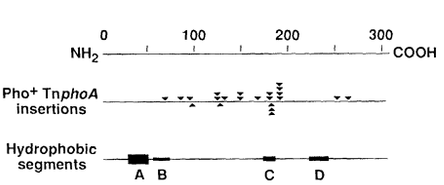

Fig. 1. Location of Tn*phoA* insertions and hydrophobic segments in MotB. Plasmid pJJ20, a pBR322 derivative carrying the *motA* and *motB* loci, served as the target for insertional mutagenesis by λ Tn*phoA*-1, following the procedures of Manoil and Beckwith (*8*). Phosphatase-positive isolates were tested by complementation analysis and genetic mapping to identify plasmids with *motB*::Tn*phoA* inserts, and their precise fusion junctions were then established by dideoxy-DNA sequence analysis with double-stranded plasmid templates and an oligonucleotide primer complementary to the NH_2-terminal coding sequence of *phoA*. Each triangle represents an independent insertion event. The identification of hydrophobic segments in MotB is based on the analysis of Stader *et al.* (*13*). The relative hydropathicity of each segment is roughly proportional to the height of the boxed region. The scale at the top gives the positions of amino acid residues in the MotB protein.

Biology Department, University of Utah, Salt Lake City, Utah 84112.

shown in Fig. 2, we examined the protease sensitivity of native MotB molecules in spheroplasts. Since proteases cannot enter spheroplasts, only those portions of MotB on the periplasmic side of the membrane should be susceptible to cleavage. Model I predicts that much of the MotB molecule should be protected from degradation, whereas model II predicts that much of it should be accessible to exogenous proteases. Two different enzymes were used in these experiments with similar results: protease V8, which cleaves at glutamic acid residues, and trypsin, which cleaves at arginine and lysine residues. The trypsin results are shown in Fig. 3.

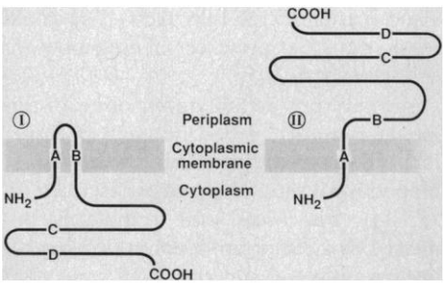

Fig. 2. Models of MotB membrane organization. Letters A to D refer to the hydrophobic segments indicated in Fig. 1.

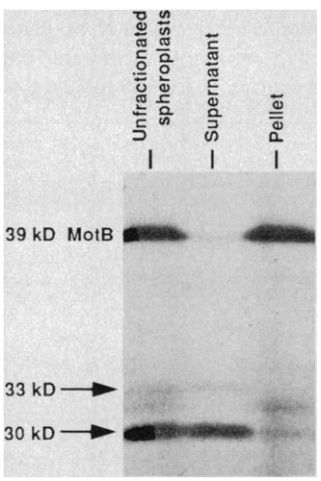

Fig. 3. MotB fragment patterns after treatment of spheroplasts with trypsin. MotB was expressed from plasmid pSYC62, a derivative of pACYC184 carrying the *motB* gene, and labeled with [^{35}S]methionine by the maxicell method (*19*) in a Mot$^+$ host strain. Spheroplasts were prepared with lysozyme and mild osmotic shock and resuspended in 20% sucrose containing 0.03*M* tris-HCl (*p*H 7.6) and 5 m*M* EDTA (*20*). Samples were treated with trypsin at 5 mg/ml for 30 minutes at 0°C. Digestion was terminated by addition of bovine pancreatic trypsin inhibitor (50 mg/ml, 10-minute incubation at 0°C). Portions of the treated samples were then centrifuged to separate intact cells and membranes from soluble extracellular material. Samples were analyzed on discontinuous 10% polyacrylamide-SDS gels. Approximate molecular sizes were determined by comparison to standard marker proteins on the same gel. Only the intact MotB protein and its two largest tryptic fragments (indicated by arrows) are shown.

Spheroplasts treated with trypsin yielded two MotB fragments in the 30- to 33-kD size range, presumably derived from one or more cleavages in the periplasmic domain (Fig. 3, left lane). Fractionation of the treated samples by centrifugation demonstrated that both fragments were present in the soluble fraction (Fig. 3, middle lane) but not in the cell pellet (Fig. 3, right lane), indicating that they had originated from the periplasmic side of the membrane. These results confirm the existence of a large periplasmic domain in MotB and show, moreover, that hydrophobic segments C and D, located in the middle of that domain, do not anchor the MotB molecule to the membrane. Thus, we propose that hydrophobic segment A initiates membrane insertion and directs the COOH-terminus of the molecule into the periplasmic compartment, as shown in model II (Fig. 2).

The probable structural relation between MotB and the flagellar motor is summarized in Fig. 4. Flagellar basal bodies are encircled by "studs," seen in freeze-fracture preparations (*15, 16*), which Khan has shown are missing in cells lacking MotA and MotB (*16*). This finding provides circumstantial evidence that MotB molecules are located around the periphery of flagellar motors. The studs may correspond to the extensive periplasmic domain of MotB indicated by our topology studies. The cytoplasmic NH_2-terminus or transmembrane portion of MotB could conceivably interact with switch proteins located at the base of the motor to produce or control rotational motion, as suggested by genetic suppression studies (*17*). However, with a single hydrophobic membrane spanning segment, it seems improbable that MotB could form a proton conductance channel, a function more likely served by MotA, which has at least four potential membrane-spanning segments (*18*). What then is the role of MotB in flagellar rotation?

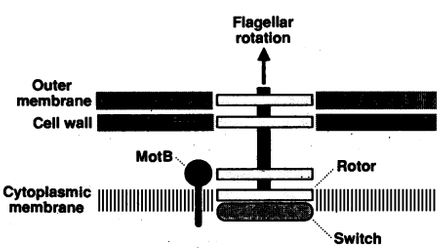

Fig. 4. Structural relation of MotB to the flagellar motor. The flagellar basal structure is comprised of four rings connected to a central rod that transmits rotational motion to the filament (*2*). The bottom ring, embedded in the cytoplasmic membrane, is most likely the rotor, whose direction of rotation is controlled by associated switch proteins. The MotB protein is probably arrayed around the periphery of the basal structure with the bulk of the molecule protruding into the periplasmic space.

Block and Berg (*7*) have shown that MotB molecules are essential components of the "force-generating units" of the flagellar motors, each of which produces a quantum increase in motor speed (torque). The force generators may correspond to the studs seen in structural studies. Berg (*5*) has pointed out that the "stator" components of the motor are most likely linked to the cell wall, providing a solid support from which they can push on the "rotor" components. We suggest that the periplasmic COOH-terminal domain of MotB may serve to anchor the force-generators to the cell wall, either through direct interaction with the cell wall or indirectly through interaction with other motor structures, which in turn are attached to the cell wall. In either case, these interactions are probably noncovalent, since force-generating units appear to be reversibly incorporated into the motor complex (*7*). According to this model, changes in motor speed would correspond to variations in the number of anchor points. More detailed structure-function studies of MotB should enable us to test these ideas and discern the functional role of this protein in bacterial motility.

REFERENCES AND NOTES

1. H. C. Berg and R. A. Anderson, *Nature (London)* **245**, 380 (1973); M. R. Silverman and M. I. Simon, *ibid.* **249**, 73 (1974).
2. M. DePamphilis and J. Adler, *J. Bacteriol.* **105**, 384 (1971).
3. M. Hilmen and M. Simon, in *Cell Motility*, R. Goldman, T. Pollard, J. Rosenbaum, Eds. (Cold Spring Harbor Laboratory, Cold Spring Harbor, NY, 1976), pp. 35–45.
4. S. H. Larsen, J. Adler, J. J. Gargus, R. W. Hogg, *Proc. Natl. Acad. Sci. U.S.A.* **71**, 1239 (1974).
5. H. C. Berg, *Nature (London)* **249**, 77 (1974).
6. J. B. Armstrong and J. Adler, *Genetics* **56**, 363 (1967).
7. S. M. Block and H. C. Berg, *Nature (London)* **309**, 470 (1984).
8. C. Manoil and J. Beckwith, *Proc. Natl. Acad. Sci. U.S.A.* **82**, 8129 (1985).
9. ———, *Science* **233**, 1403 (1986).
10. Wild-type MotB migrates in gels with an apparent molecular size of 39 to 41 kD, even though its primary sequence predicts a molecular size of 34 kD. This anomalous electrophoretic behavior is correlated with the COOH-terminus of the molecule (*13*), which is missing in the MotB-PhoA fusion proteins.
11. V. L. Miller, R. K. Taylor, J. J. Mekalonos, *Cell* **48**, 271 (1987); P. L. Boquet, C. Manoil, J. Beckwith, *J. Bacteriol.* **166**, 1663 (1987).
12. S. McCracken and E. Meighen, *J. Biol. Chem.* **255**, 2396 (1980).
13. J. Stader, P. Matsumura, D. Vacante, G. E. Dean, R. M. Macnab, *J. Bacteriol.* **166**, 244 (1986).
14. A. Boyd, G. Mandel, M. I. Simon, in *Prokaryotic and Eukaryotic Flagella*, W. B. Amos and J. G. Duckett, Eds. (Cambridge University Press, Cambridge, 1982), pp. 123–137.
15. J. W. Coulton and R. G. E. Murray, *J. Bacteriol.* **136**, 1037 (1978).

16. S. Khan, manuscript in preparation.
17. S. Yamaguchi, H. Fujita, A. Ishihara, S.-I. Aizawa, R. M. Macnab, *J. Bacteriol.* **168**, 1172 (1986).
18. G. E. Dean, R. M. Macnab, J. Stader, P. Matsumura, C. Burks, *ibid.* **159**, 991 (1984).
19. A. Sancar, A. M. Hock, W. D. Rupp, *ibid.* **137**, 692 (1979).
20. B. Witholt *et al.*, *Anal. Biochem.* **74**, 160 (1976).
21. Supported by NIH grant GM19559. We thank C. Manoil for material and intellectual support throughout this work, L. Randall for helpful experimental suggestions, H. Berg, R. Macnab, M. Manson, and P. Matsumura for thoughtful discussions and comments on an early version of the manuscript, and S. Khan for communicating results prior to publication.

17 August 1987; accepted 2 December 1987

Somatostatin Augments the M-Current in Hippocampal Neurons

SCOTT D. MOORE, SAMUEL G. MADAMBA, MARIAN JOËLS, GEORGE R. SIGGINS*

Immunocytochemical and electrophysiological evidence suggests that somatostatin may be a transmitter in the hippocampus. To characterize the ionic mechanisms underlying somatostatin effects, voltage-clamp and current-clamp studies on single CA1 pyramidal neurons in the hippocampal slice preparation were performed. Both somatostatin-28 and somatostatin-14 elicited a steady outward current and selectively augmented the noninactivating, voltage-dependent outward potassium current known as the M-current. Since the muscarinic cholinergic agonists carbachol and muscarine antagonized this current, these results suggest a reciprocal regulation of the M-current by somatostatin and acetylcholine.

IMMUNOHISTOCHEMICAL STUDIES INDICATE that prosomatostatin-derived peptides are present in intrinsic neurons of the hippocampus (*1*). These peptides include somatostatin-28 (SS28) and its cleavage fragments SS28(15–28) (SS14; somatotropin release-inhibiting factor) and SS28(1–12). Other histochemical studies have shown a profuse innervation of the hippocampus by fibers containing markers for acetylcholine (ACh) (*2*) that appear to project to the same dendritic areas of hippocampal neurons as the SS-containing fibers (*1–3*). Electrophysiological studies indicate that activation of cholinergic muscarinic receptors excites pyramidal neurons, probably by means of multiple mechanisms, including presynaptic actions, reduction of Ca^{2+} currents, and suppression of several different K^+ currents (*4–8*).

However, the function of SS14 in the hippocampus is less clear. In some studies, SS14 or SS28 elicited inhibitions and hyperpolarizations of CA1 pyramidal neurons with a reduction of input resistance (*7, 9–11*), interpreted as an increase in K^+ conductance. Excitatory effects of SS14 have also been reported (*12*). These disparate results may derive from methodological differences or from the recently described interaction of ACh and SS: when applied alone, SS elicited only inhibitory effects but enhanced the excitatory effects of ACh on cortical and hippocampal neurons (*13*). Thus, excitatory SS14 effects (*12*) could result from the presence of exogenous or endogenous ACh.

We have pursued the mechanisms of this interaction (*14*) of SS and ACh by using intracellular recording techniques in the rat hippocampal slice, prepared as described (*9, 15, 16*). The slices were completely immersed in a temperature-controlled recording chamber and superfused with standard artificial cerebrospinal fluid (ACSF) to which drugs and peptides were added (*15, 16*). Current- and voltage-clamp (*17–19*) studies were performed with an Axoclamp preamplifier. A total of 39 pyramidal neurons met criteria for lack of penetration injury (*15*). Resting membrane potentials ranged from −54 to −75 mV and averaged

S. D. Moore, S. G. Madamba, G. R. Siggins, Research Institute of Scripps Clinic, 10666 North Torrey Pines Road, La Jolla, CA 92037.
M. Joëls, Institute of Molecular Biology, State University of Utrecht, Utrecht, The Netherlands.

*To whom correspondence should be addressed.

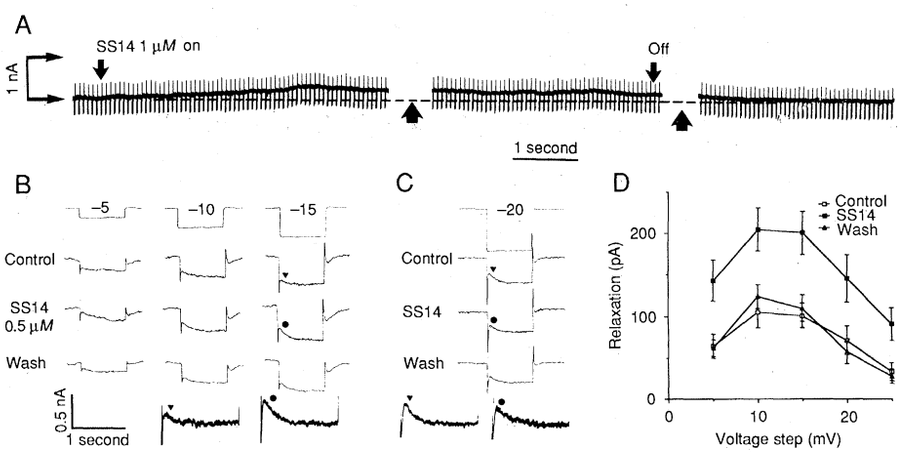

Fig. 1. Effect of SS superfusion on transmembrane currents in CA1 pyramidal neurons: single electrode voltage-clamp data were obtained with the use of potassium chloride–filled micropipettes. TTX was present in all records shown here and in Fig. 2. (**A**) In a pyramidal neuron held at resting potential (−60 mV), SS14 induces an outward (upward) current accompanied by a small increase in ionic conductance, as indicated by the 10 to 15% increase in size of the downward deflections produced by a 10-mV hyperpolarizing command pulse. Upward deflections are due to transient outward currents following command offset (probably I_A). Upward arrows indicate 5-minute gaps in the record during which current-voltage curves were generated. Downward arrows indicate duration of SS14 superfusion. (**B**) In a different neuron, hyperpolarizing voltage commands of 5, 10, and 15 mV (top trace), from a depolarized holding potential (V_H = −40 mV), produce a small inward instantaneous current followed by a slow relaxation to a greater inward steady-state level. The difference between the instantaneous and steady-state currents constitutes the M-current (*8*). Bottom two traces are enlargements (×1.7) of the relaxations obtained from control (triangle) and SS14-treated (circle) conditions during the 15-mV commands; SS14 doubles the M-current. Although only three commands are shown here, command steps of −5, −10, −15, −20, and −25 mV were used in this and all other clamped cells. (**C**) The same neuron held at −65 mV (resting potential) to elicit the Q-current relaxations (*8*) with −20-mV commands (−10- and −30-mV steps gave equivalent results). Somatostatin-14 had no effect on these current relaxations as shown by the enlargements [bottom two traces (×1.7); symbols as in (B)]. (**D**) M-current relaxations from 14 different CA1 pyramidal cells tested with SS14 or SS28 (at 0.5 to 1 μ*M*) and averaged (±SEM) over a range of voltage commands. In all cells V_H was near −40 mV. Somatostatins double the average size of the relaxations but have no detectable effect on the voltage dependency of the relaxations. The extrapolated average apparent threshold potential for these currents was about −70 mV.